BEST AVAILABLE IMAGES

Defective images within this document are accurate representations of the original documents submitted by the applicant.

Defects in the images may include (but are not limited to):

- BLACK BORDERS
- TEXT CUT OFF AT TOP, BOTTOM OR SIDES
- FADED TEXT
- ILLEGIBLE TEXT
- SKEWED/SLANTED IMAGES
- COLORED PHOTOS
- BLACK OR VERY BLACK AND WHITE DARK PHOTOS
- GRAY SCALE DOCUMENTS

IMAGES ARE BEST AVAILABLE COPY.

As rescanning documents *will not* correct images, please do not report the images to the Image Problem Mailbox.

ammonium (TEA) suggests that these agents occupy structurally homologous binding sites close to or within the mouth of the channel pore (20). Guy and Conti (27) and Hille (20) suggested an alignment of amino acid sequences where the Glu^{376} involved in TTX and STX binding in Na^+ channels is one to two positions away from the critical residue at position 449 in K^+ channels, a major site in charybdotoxin and TEA binding. Our results with the $Cys^{374} \rightarrow Tyr$ and the $Arg^{377} \rightarrow Asn$ mutants demonstrate that residues 374 to 377 are essential for binding of TTX and STX and Cd^{2+}, which would align with residues 444 to 447 of the *Shaker* K^+ channel (20, 27). This would place the TTX and STX receptor about three-eighths to three-quarters of the way into the pore, which is inconsistent with the observed lack of voltage dependence for TTX and STX binding. Identification of the residue at position 374 as critical to high-affinity toxin binding reveals the structural difference that distinguishes TTX-R and TTX-S Na^+ channel isoforms and explains the high-affinity divalent cation blockage of the RHI and the competition of divalent ions and toxin for binding. The position of this residue may require revision of the Na^+ channel pore structure suggested by homology with the K^+ channel.

Note added in proof: $Cys^{374} \rightarrow Phe$ has the same properties as $Cys^{374} \rightarrow Tyr$.

REFERENCES AND NOTES

1. R. Barchi, *Trends Neurosci.* 10, 221 (1987). R. B. Rogart, *Annu. Rev. Physiol.* 43, 711 (1981).
2. J. M. Ritchie and R. Rogart, *Rev. Physiol. Biochem. Pharmacol.* 79, 1 (1977).
3. J. F. Renaud *et al.*, *J. Biol. Chem.* 258, 8799 (1983); R. B. Rogart, *Ann. N.Y. Acad. Sci.* 479, 402 (1986).
4. C. J. Cohen *et al.*, *J. Gen. Physiol* 78, 383 (1981).
5. J. S. Trimmer and W. S. Agnew, *Annu. Rev. Physiol.* 51, 401 (1989).
6. L. L. Cribbs *et al.*, *FEES Lett.* 275, 195 (1990).
7. M. White *et al.*, *Mol. Pharmacol.* 39, 604 (1991).
8. M. Noda *et al.*, *FEBS Lett.* 259, 213 (1989).
9. H. Terlau *et al.*, *ibid.* 293, 93 (1991).
10. R. MacKinnon and G. Yellen, *Science* 250, 276 (1990).
11. R. B. Rogart *et al.*, *Proc. Natl. Acad. Sci. U.S.A.* 86, 8170 (1989).
12. To construct the mutants, we created a fragment by the polymerase chain reaction (PCR) that encompassed the Bgl II restriction sites at nucleotides (nt) 197 and 1162. The 5′ primer bound to the 5′ side of nt 197, and the 3′ primer included the Bgl II site at nt 1162 and also incorporated a single- or double-nucleotide mutation that resulted in a single amino acid change upon translation. The PCR product was ligated to a subclone (pRH11-71) of the rat cardiac Na^+ channel that spanned nt 445 to 2971. The Nsi I (nt 553) to Bam HI (nt 2956) fragment was then isolated and ligated into the expression vector pXOI. For transcription, templates were linearized with Xba I and transcribed with T7 RNA polymerase. Reaction conditions were described (6). Reagents were from Stratagene.
13. C. Frelin *et al.*, *Eur. J. Pharmacol.* 122, 245 (1986); D. DiFrancesco *et al.*, *Proc. R. Soc. London Ser. B* 223, 475 (1985). D. A. Hanck and M. F. Sheets, *J. Physiol. (London)*, in press.
14. J. Reed and W. Raftery, *Biochemistry* 15, 944 (1976). R. L. Barchi and J. B. Weigele, *J. Physiol. (London)* 295, 383 (1979); W. N. Green, L. B. Weiss, O. S. Andersen, *J. Gen. Physiol.* 89, 873 (1987).
15. L. Schild and E. Moczydlowski, *Biophys. J.* 59, 523 (1991).
16. E. Carmeliet, *ibid.* 51, 109 (1987); P. M. Vassilev *et al.*, *Am. J. Physiol.* 251, H475 (1986); R. Eickhorn *et al.*, *Pfluegers Arch.* 416, 298 (1990).
17. U. Lonnendonker, B. Neumcke, R. Stampfli, *Pfluegers Arch.* 416, 750 (1990). V. L. Salgado, J. Z. Yeh, T. Narahashi, *Ann. N.Y. Acad. Sci.* 479, 84 (1986); D. E. Patten and A. L. Goldin, *Neuron* 7, 637 (1991).
18. J. Satin, unpublished data.
19. G. Strichartz, T. Rando, G. K. Wang, *Annu. Rev. Neurosci.* 10, 237 (1987).
20. B. Hille, *Ionic Channels of Excitable Membranes* (Sinauer, Sunderland, MA, ed. 2, 1992); *Biophys. J.* 15, 615 (1975).
21. B. C. Spalding, *J. Physiol. (London)* 305, 485 (1980); P. Shrager and C. Profera, *Biochim. Biophys. Acta* 318, 141 (1973).
22. G. Strichartz *et al.*, *Ann. N.Y. Acad. Sci.* 479, 96 (1986).
23. S. L. Hu and C. Y. Kao, *J. Gen. Physiol.* 97, 561 (1991).
24. R. MacKinnon and C. Miller, *Science* 245, 1382 (1989). These authors estimated for the electrostatic interaction of charybdotoxin with the K^+ channel that a single charge alteration reduces affinity 3.5 times, which is equivalent to a free-energy change of 0.7 kcal/mol.
25. C. Brandon and J. Tooze, *Introduction to Protein Structure* (Garland, New York, 1991). For instance, the ionized hydrogen bond between Tyr^{169} of tyrosyl-tRNA synthetase and its positively charged substrate contribute about 3.7 kcal/mol.
26. D. A. Dougherty and D. A. Stauffer, *Science* 250, 1558 (1990).
27. H. R. Guy and F. Conti, *Trends Neurosci.* 13, 201 (1990).
28. Oocytes were injected with 50 to 150 ng of cRNA. Whole-oocyte current was recorded with a two-electrode voltage-clamp (TEV-200, Dagan) 2 to 5 days after injection. Recordings were made at 20° to 22°C in a flowing bath solution that consisted of 90 mM NaCl, 2.5 mM KCl, 1 mM $CaCl_2$, 1 mM $MgCl_2$, and 10 mM Hepes (pH 7.4). $CdCl_2$ was added to the bath from a 100 mM stock solution. TTX and STX were purchased from Calbiochem.
29. P. A. Pappone, *J. Physiol. (London)* 306, 377 (1980); T. Gonoi, S. J. Sherman, W. A. Catterall, *J. Neurosci.* 5, 2559 (1985).

30. We thank G. Mandel for the gift of μI cDNA; A. Fox for help with Axobasic 1.0; T. Larsen and N. Soares for technical assistance; and D. Hanck and J. Makielski for helpful discussions. Supported by NIH grants HL-20592, HL-37217, and NS 23360, a grant from the Upjohn Company, and a grant from the International Life Sciences Institute.

17 January 1992; accepted 31 March 1992

Identification of Heregulin, a Specific Activator of $p185^{erbB2}$

William E. Holmes,* Mark X. Sliwkowski, Robert W. Akita, William J. Henzel, James Lee, John W. Park, Daniel Yansura, Nasrin Abadi, Helga Raab, Gail D. Lewis, H. Michael Shepard,† Wun-Jing Kuang, William I. Wood, David V. Goeddel, Richard L. Vandlen*‡

The proto-oncogene designated *erbB2* or HER2 encodes a 185-kilodalton transmembrane tyrosine kinase ($p185^{erbB2}$), whose overexpression has been correlated with a poor prognosis in several human malignancies. A 45-kilodalton protein heregulin-α (HRG-α) that specifically induced phosphorylation of $p185^{erbB2}$ was purified from the conditioned medium of a human breast tumor cell line. Several complementary DNA clones encoding related HRGs were identified, all of which are similar to proteins in the epidermal growth factor family. Scatchard analysis of the binding of recombinant HRG to a breast tumor cell line expressing $p185^{erbB2}$ showed a single high affinity binding site [dissociation constant (K_d) = 105 ± 15 picomolar]. Heregulin transcripts were identified in several normal tissues and cancer cell lines. The HRGs may represent the natural ligands for $p185^{erbB2}$.

The $p185^{erbB2}$ protein is a 185-kD transmembrane tyrosine kinase encoded by the erbB2 proto-oncogene (1) that is similar to the epidermal growth factor (EGF) receptor (2) and the HER3, or c-*erbB3*, protein (3). Both $p185^{erbB2}$ and the EGF receptor are associated with certain human malignancies (4). In particular, overexpression of $p185^{erbB2}$ correlates with a poor prognosis in breast, ovarian, gastric, and endometrial cancers and non-small cell lung adenocarcinoma (5). EGF and transforming growth factor–α (TGF-α), which are ligands for the EGF receptor, clearly promote cell growth and transformation (1, 6). However, a similar dependence on a ligand for growth or transformation in cells expressing $p185^{erbB2}$ has not been established. Neither EGF nor TGF-α binds to or activates $p185^{erbB2}$ (7).

Evidence that $p185^{erbB2}$ may respond to exogenous ligands includes observations

Departments of Protein Chemistry, Molecular Biology and Cell Biology, Genentech, Inc., South San Francisco, CA 94080.

*W. E. Holmes and R. L. Vandlen are equal contributors to this work.
†Present address: Cenji Pharmaceuticals, San Diego, CA 92121.
‡To whom correspondence should be addressed

that some monoclonal antibodies to the extracellular domain of p185^{erbB2} can increase its tyrosine kinase activity and affect cell proliferation (*8*). There have been several reports of partially purified activities that affect p185^{erbB2} function. Two reports described an activity with a molecular size of 30 to 35 kD activating both the EGF receptor and p185^{erbB2} (*9*, *10*); a third reported that a smaller protein (8 to 24 kD) activated p185$^{c\text{-}neu}$ (the rat homolog of p185^{erbB2}) but not the EGF receptor (*11*). In contrast, we have purified and characterized a 45-kD protein, heregulin-α (HRG-α), that specifically activates tyrosine phosphorylation of p185^{erbB2}.

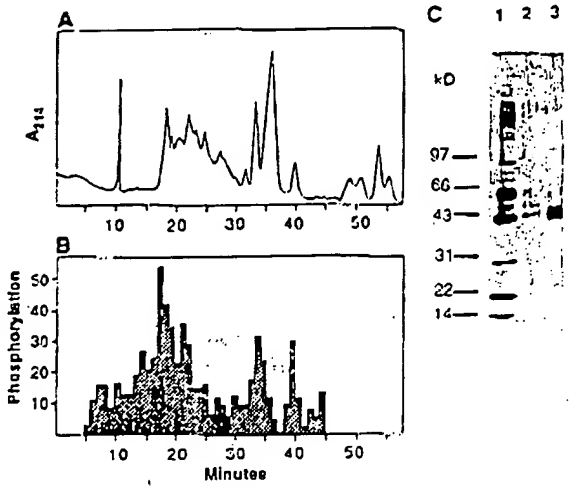

Fig. 1. Purification of heregulin from conditioned medium of MDA-MB-231 (ATCC # HTB 26) cells (*12*). (**A**) Elution of proteins (absorbance at 214 nm) from C4 reversed-phase high-performance liquid chromatography (HPLC) column. (**B**) Fractions from the HPLC column were assayed for the stimulation of tyrosine phosphorylation in p185^{erbB2}. Protein immunoblots blots were quantitated by densitometry (*12*) and the results are presented in arbitrary units. (**C**) SDS–polyacrylamide gel electrophoresis (SDS-PAGE) of fractions from the HPLC column. Proteins were visualized by silver staining. Lane 1, molecular size standards; lane 2, fraction 16 (10 μl); lane 3, fraction 17 (10 μl). The fraction with peak activity (fraction 17) contained primarily a single protein of ~45 kD, which was subjected to sequencing (*13*). The other peaks of activity contain other proteins and may be due to resolution glycosylated isoforms of HRG.

Hydropathy

Amino acids 0 200 400 600

bp −400 0 400 800 1200 1600 2000

13

(HRG-α) A_n

(HRG-β1) A_{18}

(HRG-β2) A_{13}

(HRG-β3) A_{15}

Fig. 2. Amino acid sequence of the neregulins and their relation to EGF family members. (**A**) HRG cDNAs. Hydropathy profile indicating the position of a hydrophobic domain at positions 243 to 265 (top). The coding area is boxed and cysteines are indicated (bottom). Hatching, six-cysteine EGF-like structural unit; filled box, hydrophobic segment. (♦) six potential asparagine-linked glycosylation sites (*29*); small filled box, area for possible *O*-linked glycosylation (*30*). The lengths and positions of clones 13, proHRG-α, proHRG-β1, proHRG-β2, and proHRG-β3 are shown with poly(A) tails designated (A_n). The dashed line of proHRG-β3 is a non-homologous 3′ untranslated sequence. (**B**) Amino acid sequences of the proHRGs. Amino acid sequence and alignment of three proHRG forms relative to proHRG-α. Amino acid numbers, indicated on the left, are based on proHRG-α. Shaded area, amino acids within the divergent region of the HRGs that occur in at least two forms; asterisks, COOH-terminal amino acids; overline, the 23-amino acid hydrophobic region; double dots, possible sites of glycosaminoglycan addition (*31*); triple dots, possible sites of *N*-linked glycosylation; double overline, area for possible *O*-linked glycosylation; underline, a potential nuclear targeting signal; triangles, two sites of single amino acid substitutions. Gln 38 is replaced by Arg in proHRG-β1, -β2, and -β3 and Met is replaced by Lys in proHRG-β2 at position 463. (**C**) Alignment of HRGs with human EGF family members. Shown are the EGF-like structural units of the indicated molecules. HRG sequences begin with amino acid 175 of the proforms, other proteins are numbered relative to amino acid 1 of their mature forms. Amino acids strictly conserved are shaded. Dashes, gaps in the sequence inserted for best alignment; overlines, known or putative hydrophobic domains; arrows, positions of proposed (proHRG) or known (others) COOH-terminal processing; asterisk, COOH-terminus of proHRG-β3.

screen a λgt10 cDNA library constructed with mRNA from the MDA-MB-231 cells (*14*). One hybridizing clone, which appeared to encode a precursor of HRG-α (proHRG-α), was isolated and sequenced (GenBank accession numbers M94165, M94166, M94167, and M94168). This clone (Fig. 2A) encodes a reading frame that is open at both the 5′ and 3′ ends. Related coding sequences were discovered in other λgt10 libraries from MDA-MB-231 cells (*14*) as cDNAs that encode the NH_2- and COOH-termini of proHRG-α (Fig. 2A). The cDNAs encode proteins of 640, 645, 637, and 231 amino acids, which we have termed proHRG-α, proHRG-β1, proHRG-β2, and proHRG-β3, respectively. The initiating methionine was assigned on the basis of an in-frame stop codon 444 bases upstream. Because a termination signal (TAA) exists at identical positions in both proHRG-β1 and proHRG-β2 cDNAs, a stop was assigned at a corresponding site in the sequence of proHRG-α. The four HRGs are distinguished by a variable region of 19 to 29 amino acids beginning at position 212 (Fig. 2B). The predicted amino acid sequences of proHRG-β1, proHRG-β2, and proHRG-β3 diverge from that of proHRG-α at this point and for the next 18 residues (through position 230) they share a common sequence before diverging further and losing similarity to one another. After residue 230, proHRG-β1 continues for nine more amino acids and proHRG-β2 continues for a single amino acid before both resume identity with proHRG-α at proHRG-α position 235. The proHRG-β3 cDNA encodes 11 residues beyond position

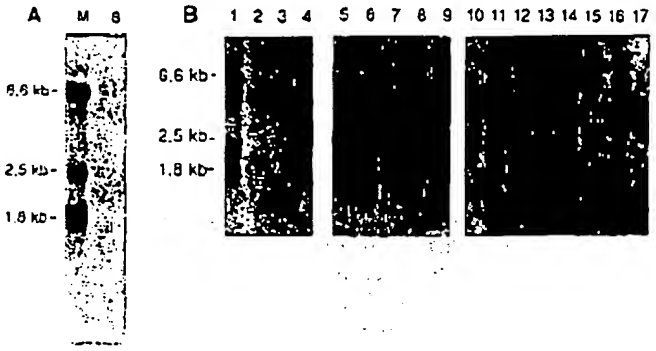

Fig. 3. Hybridization studies of human cell line and tissue mRNAs. A radiolabeled DNA fragment including proHRG-α nucleotides −90 through +610 (Fig. 2A) was hybridized with polyadenylated mRNA (5 μg) from the sources indicated below. The RNAs were first separated according to size by electrophoresis and transferred to nitrocellulose. (**A**) Human cell line mRNAs. M, MDA-MB-231; S, SK-BR-3 (ATCC # HTB 30). (**B**) Various human tissue mRNAs. Lanes 1 through 17 are breast, uterus, prostate, stomach, heart, brain, placenta, lung, liver, kidney, skeletal muscle, pancreas, ovary, testis, salivary gland, small intestine, and spleen, respectively.

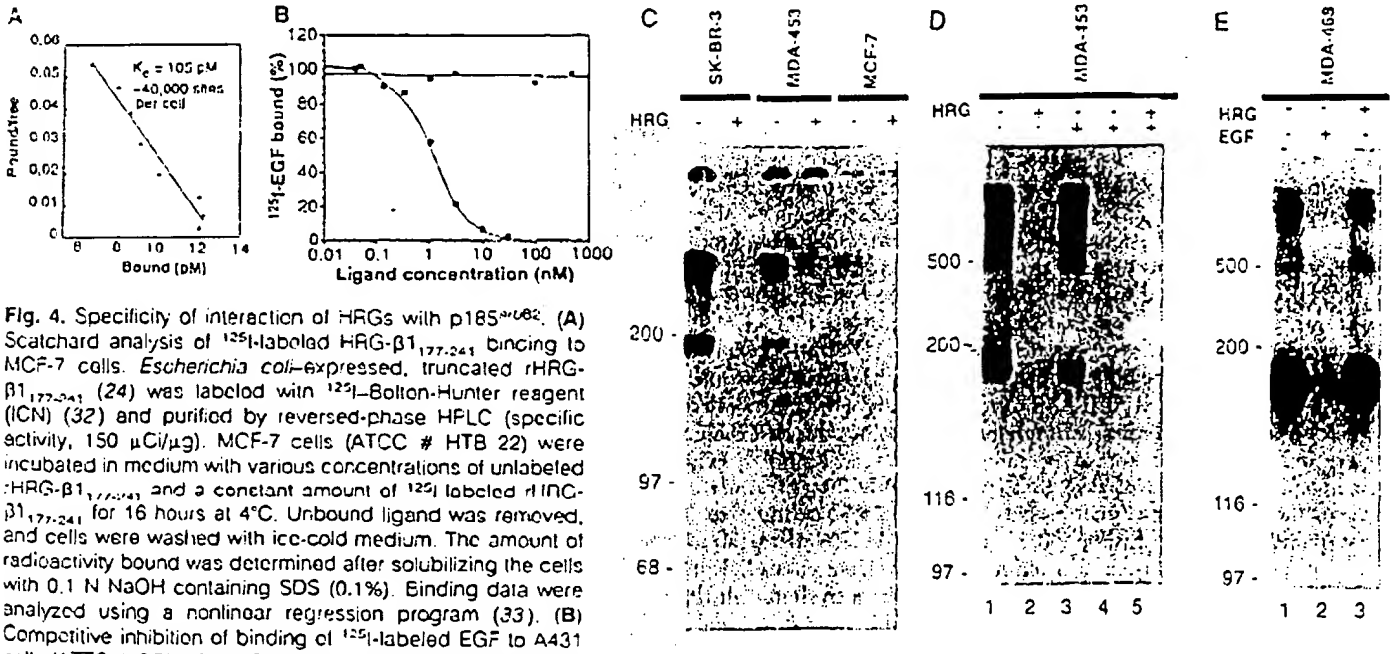

Fig. 4. Specificity of interaction of HRGs with $p185^{erbB2}$. (**A**) Scatchard analysis of ^{125}I-labeled HRG-$\beta1_{177-241}$ binding to MCF-7 cells. *Escherichia coli*–expressed, truncated rHRG-$\beta1_{177-241}$ (*24*) was labeled with ^{125}I–Bolton-Hunter reagent (ICN) (*32*) and purified by reversed-phase HPLC (specific activity, 150 μCi/μg). MCF-7 cells (ATCC # HTB 22) were incubated in medium with various concentrations of unlabeled rHRG-$\beta1_{177-241}$ and a constant amount of ^{125}I-labeled rHRG-$\beta1_{177-241}$ for 16 hours at 4°C. Unbound ligand was removed, and cells were washed with ice-cold medium. The amount of radioactivity bound was determined after solubilizing the cells with 0.1 N NaOH containing SDS (0.1%). Binding data were analyzed using a nonlinear regression program (*33*). (**B**) Competitive inhibition of binding of ^{125}I-labeled EGF to A431 cells (ATTC # CRL 1555). Cells were incubated with various concentrations of EGF (squares) or rHRG-$\beta1_{177-241}$ (circles) as described above but with ^{125}I-labeled EGF (specific activity, 200 μCi/μg). (**C**) Cross-linking of ^{125}I-labeled rHRG-$\beta1_{177-241}$ to cell lines expressing $p185^{erbB2}$. SK-BR-3, MDA-MB-453 (ATCC # HTB 131), or MCF-7 cells (2.0×10^5) were suspended in Hank's balanced salts (Gibco-BRL) and incubated with ^{125}I-labeled rHRG-$\beta1_{177-241}$ (10^6 cpm) in the absence (−) or presence (+) of unlabeled rHRG-$\beta1_{177-241}$ (100 nM) for 30 min at 22°C. Bis(sulfosuccinimidyl) suberate (Pierce) was added to the cell suspensions (final concentration, 1 mM) and the incubations were continued for 30 min. The cells were washed with tris-buffered saline (TBS) and dissolved in SDS sample buffer. Samples were run on a polyacrylamide gel (7%) and bands were visualized by autoradiography. Molecular size standards are in kilodaltons. (**D**) Cross-linking of ^{125}I-labeled rHRG-$\beta1_{177-241}$ to MDA-MB-453 cells and immunoprecipitation of the complex with antiserum to $p185^{erbB2}$. ^{125}I-labeled rHRG-$\beta1_{177-241}$ was cross-linked to MDA-MB-453 cells as described in (C) except that after the TBS wash, the cells were lysed in TBS containing Triton X-100 (0.5%). Immunoprecipitations (IP) were performed on portions of each lysate with either the guinea pig antiserum to the extracellular domain of $p185^{erbB2}$ or normal guinea pig serum as a control. Samples were prepared in SDS sample buffer, run on a polyacrylamide gel (5.5%), and visualized by autoradiography. Lane 1, cell lysate in the absence (−) of unlabeled HRG; lane 2, cell lysate in the presence (+) of HRG (100 nM); lane 3, same as lane 1 but immunoprecipitated with anti-$p185^{erbB2}$; lane 4, same as lane 1 but with normal goat serum; lane 5, same as lane 2 but immunoprecipitated with anti-$p185^{erbB2}$. (**E**) Cross-linking of ^{125}I-labeled EGF to MDA-MB-468 cells (ATCC # HTB 132). Cells were suspended in Hank's balanced salts and incubated with ^{125}I-labeled EGF (Amersham). Lane 1, cell lysate in the absence (−) of unlabeled EGF; lane 2, cell lysate in the presence (+) of EGF (100 nM); and lane 3, cell lysate in the presence (+) of 100 nM rHRG-$\beta1_{177-241}$. Cross-linking was performed as described in (C). The cells were dissolved in SDS sample buffer and run on a polyacrylamide gel (5.5%). Bands were visualized by autoradiography.

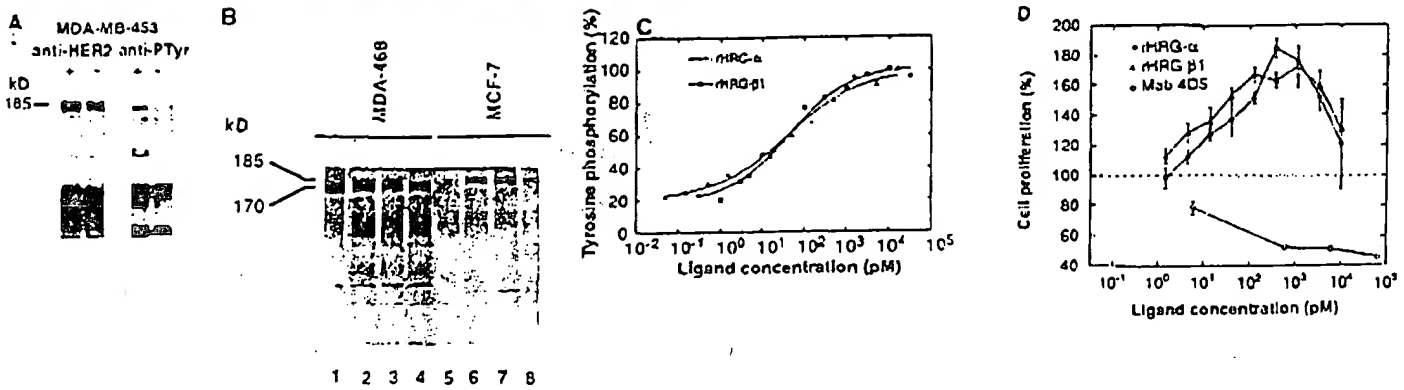

Fig. 5. Specificity and mitogenic activity of heregulins. **(A)** Immunoprecipitation of $p185^{erbB2}$ after stimulation of MDA-MB-453 cells. Cells (2.0×10^6) were suspended in 50 mM Hepes (pH 7.4) buffer containing 150 mM NaCl, 2 mM $MgCl_2$, 1 mM $MnCl_2$, and 1 mM EGTA and incubated in the presence (+) or absence (−) of rHRG-β1 (4.0 nM) (*24*) for 15 min at 22°C. Cells were lysed in the same buffer containing Triton X-100 (1.0%), 200 μM Na_3VO_4, and 10 mM EDTA. The $p185^{erbB2}$ was immunoprecipitated with guinea pig antiserum to the extracellular domain of $p185^{erbB2}$. Blots were probed with antiserum (αHER2) to a synthetic peptide corresponding to a COOH-terminal region of $p185^{erbB2}$ (*34*) or with a monoclonal antibody to phosphotyrosine (*12*). Bands at the bottom of the gel are due to the reaction of secondary antibodies with the antibodies used in the immunoprecipitation. **(B)** Stimulation of tyrosine phosphorylation in MDA-MB-468 and MCF-7 cells. Cells were treated with various concentrations of EGF, rHRG-α, or rHRG-β1 and the increase in tyrosine phosphorylation of the EGF receptor (p170) and $p185^{erbB2}$ was quantitated. Lanes 1 to 4, MDA-MB-468 cells; lanes 5 to 8, MCF-7 cells. Lane 1, human recombinant EGF (1 nM) (Upstate Biotechnology); lane 2, rHRG-α (10 nM); lane 3, rHRG-β1 (10 nM); lane 4, no ligand; lane 5, EGF (10 nM), lane 6, rHRG-α (1 nM); lane 7, rHRG-β1 (1 nM); and lane 8, no ligand. **(C)** Stimulation of tyrosine phosphorylation by rHRG-α and rHRG-β1. MCF-7 cells were incubated with various concentrations of rHRGs, and the increase in tyrosine phosphorylation of $p185^{erbB2}$ quantitated as described (*12*). The data were fit to a four-parameter nonlinear least squares equation EC_{50}'s for both rHRG-α and rHRG-β were −40 pM. **(D)** Stimulation of proliferation of SK-BR-3 cells. Cells (10^4 cells per well) were plated in 96-well microtiter plates and incubated with rHRGs or the cytostatic monoclonal antibody 4D5 (*8*) for three days before quantitation with crystal violet (*8*). Quadruplicate wells were tested at each sample concentration. Half-maximal stimulation was observed at ~20 pM.

230 before a stop codon is encountered.

Amino acid hydropathy analysis (Fig. 2A) of proHRG-α, -β1, and -β2 revealed a 23–amino acid hydrophobic region including amino acids 243 to 265 (Fig. 2) that may be a transmembrane domain or internal signal sequence. This suggests that the mature HRG-α, -β1, and -β2 molecules of 45 kD whose sequences are found on the NH_2-terminal side of this region may be derived from a transmembrane-anchored precursor molecule. The proHRG-β3 protein does not contain this hydrophobic region and is predicted not to be membrane-bound. Unlike typical signal sequences the NH_2-terminal amino acids of these proteins are not hydrophobic. Instead, the first 23 amino acids are dominated by charged residues and contain a sequence (GKKKER; residues 13 to 18) that closely resembles the consensus sequence motif for nuclear targeting (*15*).

The NH_2-terminus determined for HRG-α (*13*) begins with serine 2 encoded by the cDNA. Analysis of COOH-terminal peptides (*13*) of the mature HRGs indicated that none of the COOH-termini extended beyond HRG-α position 241 (Fig. 2C). Thus, the mature HRGs probably range in size from 228 to 241 amino acids with a predicted molecular size of ~26 kD. Post-translational modification occurring at predicted glycosylation sites could account for the difference between the predicted and observed (~45 kD by SDS-PAGE under reducing conditions) molecular sizes of the HRGs.

The HRGs, with the exception of HRG-β3, each contain twelve cysteine residues (Fig. 2), 6 of which are clustered within a 40–amino acid segment adjacent to the putative transmembrane region. The characteristic number and relative positions of these cysteines, as well as the strict conservation of two glycines and an arginine residue within this region (Fig. 2C), establish the HRGs as members of the EGF family (*16*). Between the first and sixth cysteines the HRGs are most similar (45%) to heparin-binding EGF-like growth factor (HB-EGF) (*17*). In this same region they are 35% identical to amphiregulin (AR) (*18*), 32% identical to TGF-α (*19*), and 27% identical to EGF (*16*). Outside of this EGF motif there is little similarity between HRGs and other members of the EGF family. EGF, AR, HB-EGF, and TGF-α are all derived from membrane-anchored precursors that are cleaved on both sides of the EGF structural unit to yield 50– to 84–amino acid mature proteins (*16–19*). Like the EGF family members, the HRGs appear to be derived from a membrane-bound precursor but require only a single cleavage, COOH-terminal to the cysteine cluster, to produce mature proteins.

The expression of HRG mRNA in two breast carcinoma cell lines was studied by Northern (RNA) blot analysis with a cDNA probe encoding the NH_2-terminal portion of proHRG-α. Three major bands, representing transcripts of 6.6, 2.5, and 1.8 kb, were detected in mRNA from MDA-MB-231 cells (Fig. 3A). No HRG mRNA was detected in the SK-BR-3 cell line, which overexpresses $p185^{erbB2}$.

The various cDNA clones were mapped to the MDA-MB-231 transcripts by hybridization with a panel of synthetic oligonucleotide probes (*20*). The NH_2-terminal region common to all four HRG subtypes hybridized with all three transcripts. Oligonucleotides corresponding to the sequence of HRG-α hybridized predominantly with the 6.6- and 2.5-kb transcripts, and oligonucleotides corresponding to the sequence of HRG-β hybridized more strongly with the 1.8-kb transcript. The common hydrophobic and COOH-terminal encoding regions of HRG-α, -β1, and -β2 mRNAs hybridized with only the 6.6-kb and 2.5-kb transcripts, whereas the divergent 3′ region of HRG-β3 hybridized only with the 1.8-kb message (*21*).

Various human tissues were also examined for the presence of HRG mRNA (Fig. 3B). Transcripts were found in breast, ovary, testis, prostate, heart, skeletal muscle, lung, liver, kidney, salivary gland, small intestine, brain, and spleen but not in stomach, pancreas, uterus, or placenta. Although most of these tissues contained the same three classes of transcripts as the MDA-MB-231 cells, only the 6.6-kb message was observed in heart and skeletal muscle. In brain a single transcript of 2.2 kb was detected and in testis the 6.6-kb transcript was present along with others of 2.2, 1.9, and 1.5 kb. The tissue-specific expres-

sion pattern observed for HRG differed from that of p185^{erbB2}. Adult liver, spleen, and brain contain HRG but not p185^{erbB2} transcripts (22), whereas stomach, pancreas, uterus, and placenta contain p185^{erbB2} transcripts (23) but lack HRG mRNA.

To characterize physical and functional properties of the HRGs, recombinant proteins were produced. Recombinant HRG-α (rHRG-α) and recombinant HRG-β1 (rHRG-β1) representing mature (~45 kD) processed forms of proHRGs were purified from the conditioned medium of mammalian cells transfected with full-length cDNA clones (24). Truncated versions of rHRG-α (rHRG-$\alpha_{177-239}$) and rHRG-β1 (rHRG-$\beta1_{177-241}$) were produced in *Escherichia coli* (24). Direct binding of rHRG-$\beta1_{177-241}$ to p185^{erbB2} was demonstrated in several ways. Scatchard analysis showed a single class of high-affinity binding sites (K_d of 105 ± 15 pM) on the surface of MCF-7 cells (Fig. 4A), a cell line that expresses low levels of p185^{erbB2} (25). Similar K_d's were observed with MDA-MB-453 cells and SK-BR-3 cells (26). Whereas unlabeled EGF fully competed with ^{125}I-labeled EGF for binding to A431 human epidermoid carcinoma cells [2 × 10^6 receptors per cell (27)], rHRG-$\beta1_{177-241}$ (at concentrations up to 500 nM) failed to compete (Fig. 4B), indicating that rHRG-$\beta1_{177-241}$ does not bind to the EGF receptor. Cross-linking of ^{125}I-labeled rHRG-$\beta1_{177-241}$ to receptors on the surface of SK-BR-3 cells, MDA-MB-453 cells, and MCF-7 cells, which express high, medium, and low amounts of p185^{erbB2}, respectively (25), revealed an ~190-kD complex, consistent with the size expected of a complex between p185^{erbB2} and the rHRG-$\beta1_{177-241}$ protein [7.9 kD (26)] (Fig. 4C). The amount of this complex was proportional to the amount of p185^{erbB2} expression on the various cell lines examined. Because of the small size of rHRG-$\beta1_{177-241}$ it is difficult to determine the precise stoichiometry of the ~190-kD complex. As has been observed with EGF and the EGF receptor (28) (Fig. 4E) other larger complexes were present that may be oligomeric forms of cross-linked p185^{erbB2} and rHRG-$\beta1_{177-241}$. These complexes were eliminated when unlabeled rHRG-$\beta1_{177-241}$ was added to the cells before cross-linking. The identity of the cross-linked material was confirmed by immunoprecipitation. Polyclonal antisera from guinea pig to the extracellular domain of p185^{erbB2} precipitated cross-linked complexes from MDA-MB-453 cells that comigrated during SDS-PAGE under reducing conditions with cross-linked complexes that had not been immunoprecipitated (Fig. 4D). Irrelevant guinea pig antisera yielded no complexes after precipitation. Cross-linking of ^{125}I-labeled EGF to EGF receptors on the surface of MDA-MB-468 cells was abolished by addition of excess unlabeled EGF and unaffected by addition of rHRG-$\beta1_{177-241}$ (Fig. 4E), thus further substantiating that rHRG-$\beta1_{177-241}$ does not compete for EGF binding to the EGF receptor.

We immunoprecipitated p185^{erbB2} from MDA-MB-453 cells (which contain moderate amounts of p185^{erbB2} but no detectable EGF receptor) (25) and detected the protein by immunoblotting with antibodies to phosphotyrosine. The p185^{erbB2} protein was phosphorylated after treatment with ~45-kD rHRG-β1 purified from mammalian cells (Fig. 5A), or similarly derived ~45-kD rHRG-α (26). The same result was obtained with MCF-7 cells, but a less intense signal was observed (26). Whereas both ~45-kD rHRG-α and ~45-kD rHRG-β1 stimulated p185^{erbB2} phosphorylation in MCF-7 cells, neither protein activated phosphorylation of the EGF receptor in MDA-MB-468 cells (which contain large amounts of the EGF receptor) (25) (Fig. 5B). This result is consistent with the fact that rHRG-$\beta1_{177-241}$ bound directly to p185^{erbB2} (Fig. 4, A and D) and did not compete for binding to the EGF receptor (Fig. 4, B and E).

The relative ability of ~45-kD rHRG-α and -β1 to induce phosphorylation of p185^{erbB2} was evaluated. Both proteins stimulated phosphorylation of p185^{erbB2} on MCF-7 cells with a medium effective concentration (EC_{50}) of ~40 pM (Fig. 5C). Both rHRG-α and -β1 stimulated the growth of SK-BR-3 cells with an EC_{50} of ~20 pM (Fig. 5D). Optimal stimulation by either molecule was observed at ~400 pM; higher concentrations up to 10 nM were less effective in stimulating cell growth. A p185^{erbB2} ligand has been described that inhibits the growth of SK-BR-3 cells (9).

The heregulin family described here shows the characteristics expected of a ligand that interacts specifically with p185^{erbB2}. The molecular properties of the heregulins are different from those of other ligands that have been described (9–11) in that they have a different size, they stimulate rather than inhibit the proliferation of breast cancer cells in monolayer culture, and they increase tyrosine phosphorylation of p185^{erbB2} but not of the EGF receptor.

REFERENCES AND NOTES

1. Y. Yarden and A. Ullrich, *Annu. Rev. Biochem.* 57, 443 (1988).
2. A. Ullrich *et al.*, *Nature* 309, 418 (1984).
3. M. H. Kraus, W. Issing, T. Miki, N. C. Popescu, S. A. Aaronson, *Proc. Natl. Acad. Sci. U.S.A.* 86, 9193 (1989).
4. L. Coussens *et al.*, *Science* 230, 1132 (1985); C. R. King, M. H. Kraus, S. A. Aaronson, *ibid.* 229, 974 (1985).
5. D. J. Slamon *et al.*, *ibid.* 235, 177 (1987); D. J. Slamon *et al.*, *ibid.* 244, 707 (1989); Y. Yonemura *et al.*, *Cancer Res.* 51, 1034 (1991); M. P. Borst *et al.*, *Gynecol. Oncol.* 38, 364 (1990); J. A. Kern *et al.*, *Cancer Res.* 50, 5184 (1990).
6. S. A. Aaronson, *Science* 254, 1146 (1991); H. Riedel, S. Massoglia, J. Schlessinger, A. Ullrich, *Proc. Natl. Acad. Sci. U.S.A* 85, 1477 (1988).
7. Y. Yarden and R. A. Weinberg, *Proc. Natl. Acad. Sci. U.S.A* 86, 3179 (1989); R. Goldman, R. B. Levy, E. Peles, Y. Yarden, *Biochemistry* 29, 11024 (1990).
8. R. M. Hudziak *et al.*, *Mol. Cell. Biol.* 9, 1165 (1989); J. C. Sarup *et al.*, *Growth Regulation* 1, 72 (1991); R. Kumar, H. M. Shepard, J. Mendelsohn, *Mol. Cell. Biol.* 11, 979 (1991); G. K. Scott *et al.*, *J. Biol. Chem.* 266, 14300 (1991).
9. R. Lupu *et al.*, *Science* 249, 1552 (1990).
10. Y. Yarden and E. Peles, *Biochemistry* 30, 3543 (1991).
11. K. Dobashi *et al.*, *Proc. Natl. Acad. Sci. U.S.A* 88, 8582 (1991); J. Davis *et al.*, *Biochem. Biophys. Res. Commun.* 179, 1536 (1991).
12. Heregulin was purified from medium conditioned by MDA-MB-231 breast cancer cells (ATCC # HTB 26) grown on Percell Biolytica microcarrier beads (Hyclone Labs). The medium (10 liters) was concentrated ~25-fold by filtration through a membrane (10-kD cutoff) (Millipore) and clarified by centrifugation and filtration through a filter (0.22 μm). The filtrate was applied to a heparin Sepharose column (Pharmacia) and the proteins were eluted with steps of 0.3, 0.6, and 0.9 M NaCl in phosphate-buffered saline. Activity in the various chromatographic fractions was measured by quantitating the increase in tyrosine phosphorylation of p185^{erbB2} in MCF-7 breast tumor cells (ATCC # HTB 22). MCF-7 cells were plated in 24-well Costar plates in F12 (50%) Dulbecco's minimum essential medium (50%) containing serum (10%) (10^5 cells per well), and allowed to attach for at least 24 hours. Prior to assay, cells were transferred into medium without serum for a minimum of 1 hour. Column fractions (10 to 100 μl) were incubated for 30 min. at 37°C. Supernatants were then aspirated and the reaction was stopped by the addition of SDS-PAGE sample buffer (100 μl). Samples were heated for 5 min. at 100°C, and portions (10 to 15 μl) were applied to a tris-glycine gel (4 to 20%) (Novex). After electrophoresis, proteins were electroblotted onto a polyvinylidenedifluoride (PVDF) membrane and then blocked with bovine serum albumin (5%) in tris-buffered saline containing Tween-20 (0.05%) (TBST). Blots were probed with a monoclonal antibody (1:1000 dilution) to phosphotyrosine (Upstate Biotechnology) for a minimum of 1 hour at room temperature. Blots were washed with TBST, probed with an antibody to mouse immunoglobulin G conjugated to alkaline phosphatase (Promega) (diluted 1:7500) for a minimum of 30 min at room temperature. Reactive bands were visualized with 5-bromo-4-chloro-3-indoyl-1-phosphate and nitro-blue tetrazolium. Immunoblots were scanned with a Scan Jet Plus (Hewlett-Packard) densitometer. Signal intensities for unstimulated MCF-7 cells were 20 to 30 units. Fully stimulated p185^{erbB2} yielded signals of 180 to 200 units. The 0.6 M NaCl pool, which contained most of the activity, was applied to a polyaspartic acid (PolyLC) column equilibrated in 17 mM sodium phosphate (pH 6.8) containing ethanol (30%). A linear gradient from 0.3 M to 0.6 M NaCl in the equilibration buffer was used to elute bound proteins. A peak of activity (at ~0.45 M NaCl) was further fractionated on a C4 reversed-phase column (SynChropak RP-4) equilibrated in buffer containing TFA (0.1%) and acetonitrile (15%). Proteins were eluted from this column with an acetonitrile gradient from 25 to 40% over 60 min. Fractions (1 ml) were collected, assayed for activity (Fig. 1B), and analyzed by SDS-PAGE on tris-glycine gels (4–20%, Novex).
13. HPLC-purified HRG-α was digested with lysine C in SDS (0.1%), 10 mM dithiothreitol, 0.1 M NH_4HCO_3 (pH 8.0) for 20 hours at 37°C and the resultant fragments were resolved on a Synchrom C4 column (4000 Å, 0.2 by 10 cm). The column was equilibrated in 0.1% TFA and eluted with a 1-propanol gradient in 0.1% TFA [W. J. Henzel, J. T. Stults, C. Hsu, D. W. Aswad, *J. Biol. Chem.* 264, 15905 (1989)]. Peaks from the chromatographic

run were dried under vacuum and sequenced. One of the peptides (eluting at ~24% 1-propanol) gave the sequence (A)AEKEKTF[C]VNGGEXFM-VKDLXNP. Residues in brackets were uncertain and an X represents a cycle in which it was not possible to identify the amino acid. The initial yield was 8.5 pmol and the sequence did not correspond to any known protein. Residues 1, 9, 15, and 22 were later identified in the cDNA sequence as cysteine. Direct sequencing of the ~45-kD band from a gel that had been overloaded and blotted onto a PVDF membrane revealed a low abundance sequence XEXKE[G][R]GK[G]K[G]-KKKEXGXG[K] with a very low initial yield (0.2 pmol). This corresponded to residues 2 to 22 of proHRG-α (Fig. 2), suggesting that serine 2 is the NH_2-terminus of proHRG-α. Although the NH_2-terminus was blocked, we have observed that occasionally a small amount of a normally blocked protein may not be post-translationally modified. The NH_2-terminal assignment was confirmed by mass spectrometry of the protein after digestion with cyanogen bromide. The COOH-terminus of the isolated protein has not been definitely identified; however, by mixture sequencing of proteolytic digests, the mature sequence does not appear to extend past residue 241. Abbreviations for amino acid residues are: A, Ala; C, Cys; D, Asp; E, Glu; F, Phe; G, Gly; H, His; I, Ile; K, Lys; L, Leu; M, Met; N, Asn; P, Pro; Q, Gln; R, Arg; S, Ser; T, Thr; V, Val; W, Trp; and Y, Tyr.

14. An oligo(dT)-primed λgt10 [T. V. Huynh, R. A. Young, R. W. Davis, *λgt10 and λgt11 DNA Cloning Techniques: A Practical Approach*, D. Glover, Ed. (IRC Press, Oxford, 1984)] cDNA library was constructed [U. Gubler and B. J. Hoffman, *Gene* 25, 263 (1983)] with mRNA purified [J. M. Chirgwin, A. E. Przybyla, R. J. MacDonald, W. J. Rutter, *Biochemistry* 18, 5294 (1979)] from MDA-MB-231 cells. The following eightfold degenerate antisense deoxyoligonucleotide encoding the 13-amino acid sequence AEKEKTFCVNGGE (*13*) was designed on the basis of human codon frequency optima [R. Lathe, *J. Mol. Biol.* 183, 1 (1985)] and chemically synthesized: 5'-CTCGCC(G or T)CC(A or G)TTCAC(A or G)CA-GAAGGTCTTCTCCTTCTCAGC-3'. For the purpose of probe design a cysteine was assigned to an unknown residue in the amino acid sequence (*13*). The probe was labeled by phosphorylation and hybridized under low-stringency conditions to the cDNA library. The proHRG-α protein was identified in this library. HRG-β1 cDNA was identified by probing a second oligo(dT)-primed λgt10 library made from MDA-MB-231 cell mRNA with sequences derived from both the 5' and 3' ends of proHRG-α. Clone 13 (Fig. 2A) was a product of screening a primed (5'-CCTCGCTCCTCTTCT-TGCCCTTC-3' primer, proHRG-α antisense nucleotides 33 to 56) MDA-MB-231 λgt10 library with 5' HRG-α sequence. We used a sequence corresponding to the 5' end of clone 13 as the probe, to identify proHRG-β2 and proHRG-β3 in a third oligo(dT)-primed λgt10 library derived from MDA-MB-231 cell mRNA. Two cDNA clones encoding each of the four HRGs were sequenced [F. Sanger, S. Milkon, A. R. Coulson, *Proc. Natl. Acad. Sci. U.S.A.* 74, 5463 (1977)]. Another cDNA designated clone 84 has an amino acid sequence identical to proHRG-β2 through amino acid 420. A stop codon at position 421 is followed by a different 3'-untranslated sequence.

15. B. Roberts, *Biochim. Biophys. Acta*, 1008, 263 (1989).
16. G. I. Bell *et al.*, *Nucleic Acids Res.* 14, 8427 (1986).
17. S. Higashiyama, J. A. Abraham, J. Miller, J. C. Fiddes, M. Klagsbrun, *Science* 251, 936 (1991).
18. G. D. Plowman *et al.*, *Mol. Cell. Biol.* 10, 1969 (1990).
19. R. Derynck, A. B. Roberts, M. E. Winkler, E. Y. Chen, D. V. Goeddel, *Cell* 38, 287 (1984).
20. Fourteen oligonucleotide probes to the conserved and divergent regions of the proHRGs were chemically synthesized. RNA blot hybridizations were done with individual radiolabeled probes on portions (5 μg) of MDA-MB-231 cell poly(A)$^+$ mRNA that were separated according to size by gel electrophoresis and transferred to nitrocellulose.
21. J. Lee and W. Wood, unpublished data.
22. Y. Yonemura *et al.*, *Cancer Res.* 51, 1034 (1991); S. Jain *et al.*, *Int. J. Cancer* 48, 668 (1991); N. R. Lemoine *et al.*, *Br. J. Cancer* 64, 79 (1991); J. Yokota *et al.*, *Oncogene* 2, 283 (1988).
23. M. F. Press, C. Cordon-Cardo, D. J. Slamon, *Oncogene* 5, 953 (1990).
24. The proHRG-α and proHRG-β1 cDNAs were spliced into Epstein Barr virus–derived expression vectors containing a cytomegalovirus promotor. The rHRGs were purified [essentially as described (*12*)] from the serum-free conditioned medium of stably transfected CEN4 cells [human kidney 293 cells (ATCC no. CRL 1573) expressing the Epstein Barr virus EBNA-1 transactivator]. Amino acid sequence analysis of proteolytic digestion products from rHRG-α and -β1 confirmed their similarity to naturally derived HRGs, which appear to be cleaved versions of proHRGs (W. Henzel, unpublished data). A factor causing phosphorylation of $p185^{c\text{-}erbB2}$ was derived from conditioned medium of transfected COS7 monkey kidney cells transiently transfected with constructs expressing full-length proHRG-α, -β1, or -β2 (*21*). However, similar constructs expressing proHRG-β3 failed to yield activity, suggesting that the hydrophobic domain missing in proHRG-β3 may be necessary for delivery of the precursor to the cell surface and cleavage to form the mature protein. Truncated versions of proHRG-α [63 amino acids, serine 177 to tyrosine 239, (rHRG-$\alpha_{177-239}$)] and proHRG-β1 [68 amino acids, serine 177 to tyrosine 241 (rHRG-$\beta1_{177-241}$)] (Fig. 2B), each encoding the EGF structural unit and immediate flanking regions, were expressed in *E. coli*. These proteins were purified from the periplasmic space and culture broth of cells transformed with expression vectors designed to secrete recombinant proteins [C. N. Chang, M. Rey, B. Bochner, H. Heyneker, G. Gray, *Gene* 55, 189 (1987)] and stimulated tyrosine phosphorylation of $p185^{c\text{-}erbB2}$ with an EC_{50} of ~40 pM (*26*). Thus, the biological activity of HRG appears to reside in the EGF-like domain of the protein, and carbohydrate moieties are apparently not essential for activity in this assay. Purified rHRG-$\beta1_{177-241}$ was used for binding and cross-linking experiments.
25. G. Lewis and H. M. Shepard, unpublished data.
26. M. X. Sliwkowski, unpublished data.
27. N. E. Davidson, E. P. Gelman, M. E. Lippman, R. B. Dickson, *Mol. Endo.* 1, 216 (1987).
28. Y. Yarden and J. Schlessinger, *Biochemistry* 26, 1434 (1987).
29. R. Winzler, *Hormonal Proteins and Peptides*, C. H. Li, Ed. (Academic Press, New York, 1973), pp. 1–15.
30. R. D. Marshall, *Biochem. Soc. Symp.* 40, 17 (1974).
31. L. A. Goldstein *et al.*, *Cell* 56, 1063 (1989).
32. A. E. Bolton and W. M. Hunter, *Biochem. J.* 133, 529 (1973).
33. P. Munson and D. Rodbard, *Anal. Biochem.* 107, 220 (1980).
34. R. M. Hudziak, J. Schlessinger, A. Ullrich, *Proc. Natl. Acad. Sci. U.S.A.* 84, 7159 (1987).

35. We thank S. Smigelski and G. Polastri for cell culture; J. Bouroll and J. Stults for mass spectrometry; P. Jhurani, M. Vasser, and P. Ng for DNA synthesis; A. Lee for DNA sequencing; B. Fendly for antibodies; G. Bennett for labeling of HRG; D. Reilly for *E. coli* fermentations; and M. Carver, I. Figari, C. Kotts, and J. Lofgren for biological assays.

9 March 1992; accepted 24 April 1992

Less Mortality but More Relapses in Experimental Allergic Encephalomyelitis in CD8$^{-/-}$ Mice

Dow-Rhoon Koh, Wai-Ping Fung-Leung, Alexandra Ho, Dawn Gray, Hans Acha-Orbea, Tak-Wah Mak

Mice lacking in CD8 were generated from homologous recombination in embryonal stem cells at the CD8 locus and bred with the experimental allergic encephalomyelitis (EAE)-susceptible PL/J H-2^u through four backcross generations to investigate the role of CD8$^+$ T cells in this model of multiple sclerosis. The disease onset and susceptibility were similar to those of wild-type mice. However, the mutant mice had a milder acute EAE, reflected by fewer deaths, but more chronic EAE, reflected by a higher frequency of relapse. This suggests that CD8$^+$ T lymphocytes may participate as both effectors and regulators in this animal model.

Experimental allergic encephalomyelitis is a T cell–dependent, induced autoimmune disease and is considered an instructive experimental model for the human demyelinating disease multiple sclerosis because of the pathological and clinical similarities between the two. EAE can be induced in a variety of animals by injection of myelin basic protein (MBP), proteolipid protein (PLP), or peptide fragments of the proteins along with an adjuvant (*1–3*).

The role of T cells in EAE has been amply substantiated by immunological approaches such as neonatal thymectomy (*4*) and T lymphocyte depletion with antibodies (*5, 6*) as well as by the ability to transfer disease into a naïve mouse with activated CD4$^+$ T cells (*7–12*). Depletion of CD4$^+$ and CD8$^+$ T cell subsets implicates the CD4$^+$ cells as the main disease-initiating component (*5, 6, 13, 14*). Studies involving antibody depletion in rats (*13, 14*) have not implicated CD8$^+$ cells as having a

D.-R. Koh, W.-P. Fung-Leung, A. Ho, D. Gray, T.-W. Mak, Ontario Cancer Institute, Departments of Medical Biophysics and Immunology, University of Toronto, Princess Margaret Hospital, 500 Sherbourne Street, Toronto, Canada M4X 1K9
H. Acha-Orbea, Ludwig Institute for Cancer Research, Lausanne Branch, 1066 Epalinges, Switzerland.